

Dramatic increase in lymph node dendritic cell number during infection by the mouse mammary tumor virus occurs by a CD62L-dependent blood-borne DC recruitment

Pilar Martín, Sara Ruiz Ruiz, Gloria Martínez del Hoyo, Fabienne Anjuère, Héctor Hernández Vargas, María López-Bravo, and Carlos Ardavín

Despite the information dealing with the differential phenotype and function of the main mouse dendritic cell (DC) subpopulations, namely, CD8 α ⁻ and CD8 α ⁺ DCs, their origin and involvement in antiviral immune responses *in vivo* are still largely unknown. To address these issues, this study used the changes occurring in DC subpopulations during the experimental infection by the Swiss (SW) strain of the mouse mammary tumor virus (MMTV). MMTV(SW) induced an 18-fold increase in lymph node DCs, which can be blocked

by anti-CD62L treatment, concomitant with the presence of high numbers of DCs in the outer cortex, in close association with high endothelial venules. These data suggest that the DC increase caused by MMTV(SW) infection results from the recruitment of blood-borne DCs via high endothelial venules, by a CD62L-dependent mechanism. In addition, skin sensitization assays indicate that MMTV(SW) infection inhibits epidermal Langerhans cell migration to the draining lymph node. Moreover, data on the kinetics of

MMTV(SW)-induced expansion of the different DC subsets support the hypothesis that CD8⁻ and CD8⁺ DCs represent different maturation stages of the same DC population, rather than myeloid- and lymphoid-derived DCs, respectively, as previously proposed. Finally, the fact that DCs were infected by MMTV(SW) suggests their participation in the early phases of infection. (Blood. 2002;99:1282-1288)

© 2002 by The American Society of Hematology

Introduction

Dendritic cells (DCs) play a central role in the immune system due to their main function as initiators and regulators of antigen-specific antiviral T-cell responses and in the pathogenesis of a variety of viruses, such as human immunodeficiency virus (HIV), cytomegalovirus, measles virus, herpes virus, influenza virus, and respiratory syncytial virus.¹ However, little is known about the subpopulations of DCs involved in antiviral responses, the kinetics of the variations of DC subpopulations, and, importantly, the mechanisms of recruitment of DCs to the lymph nodes (LNs) during inflammatory responses driven by viral infections. On the other hand, despite the available information dealing with the phenotype and function of the 2 main mouse DC subsets, namely, CD8⁻ and CD8⁺ DCs, their involvement in antiviral immune responses *in vivo* as well as their functional relationships and origin remain largely unknown.

Over the last years CD8⁻ and CD8⁺ DCs have been ascribed to the myeloid and lymphoid lineages, respectively, and consequently considered as independent DC categories.¹ However, more recently 2 reports from our group and Dr Weissman's laboratory (Stanford University) have described the generation of both CD8⁻ and CD8⁺ DCs from a common lymphoid precursor² or from either myeloid- or lymphoid-committed precursors.³ These results suggest that in fact CD8⁻ and CD8⁺ DCs might not represent independent cell types, and in this sense we have previously reported that migration- or CD40L ligation-induced Langerhans cell (LC) maturation involved CD8 up-regulation.^{4,5} In these reports, which have been

confirmed by a recent article by Merad et al,⁶ we showed that the LN-restricted CD8^{int} DC population derived from LCs.^{4,5} On the basis of these previous data on LN DCs and using the dramatic changes occurring in the draining popliteal LNs (PO-LNs) after infection by the Swiss (SW) strain of the mouse mammary tumor virus (MMTV),⁷ we have extensively analyzed the mechanisms of DC recruitment during the inflammatory responses induced by a viral infection as well as the relationships between the different DC subsets involved. The results presented here indicate that MMTV(SW) induces a strong migration of blood-borne CD8⁻ DCs to the PO-LNs via high endothelial venules (HEVs), providing direct evidence of DC recruitment to the LNs during an *in vivo* viral infection-driven inflammatory process. Moreover, our data strongly suggest that LN CD8⁺ DCs originate as the result of CD8 up-regulation by LN CD8⁻ DCs, supporting the view that these subsets represent different physiologic states of the same DC population. Finally, the fact that DCs become infected by MMTV(SW) suggest their participation in the immune response against this virus.

Materials and methods

Experimental infection with MMTV(SW)

The MMTV(SW) was purified from milk and titered as described previously.⁸ Eight- to 10-week-old BALB/c mice were given a 10- μ L injection

From the Department of Cell Biology, Faculty of Biology, Complutense University, Madrid, Spain.

Submitted August 23, 2001; accepted October 11, 2001.

Supported by the European Commission (grant no. QLRT-1999-00276), the Comunidad de Madrid of Spain (grant no. 08.1/0076/2000), and the Ministerio de Ciencia y Tecnología of Spain (grant no. BOS 2000-0558).

Reprints: Carlos Ardavín, Dept of Cell Biology, Faculty of Biology, Complutense University, 28040 Madrid, Spain; e-mail: ardavin@bio.ucm.es.

The publication costs of this article were defrayed in part by page charge payment. Therefore, and solely to indicate this fact, this article is hereby marked "advertisement" in accordance with 18 U.S.C. section 1734.

© 2002 by The American Society of Hematology

of MMTV(SW), corresponding approximately to 10^9 virus particles, in the hind footpad. At the indicated times, the PO-LNs and for polymerase chain reaction (PCR) studies also the mesenteric LNs (MS-LNs), were removed and processed as indicated below. In this study mice were analyzed at days 1, 3, 6, and 10 after virus injection, corresponding to the key phases of virus infection, that is, the peak of B-cell polyclonal activation, response of T cells specific for the superantigen encoded by MMTV(SW), MMTV(SW)-infected B-cell differentiation into extrafollicular plasmablasts, and decline of the overall immune response against MMTV(SW) in the PO-LNs, respectively.^{7,9}

LN DC isolation

The PO-LN and MS-LN cell suspensions were filtered through a stainless-steel sieve and washed twice in phosphate-buffered saline (PBS) solution supplemented with 3% fetal calf serum (FCS) and 5 mM EDTA (PBS-EDTA-FCS). The cells were then resuspended in cold isosmotic Optiprep solution (Nyegaard Diagnostics, Oslo, Norway), pH 7.2, density 1.061 g/cm^3 , containing 5 mM EDTA to dissociate DC-lymphocyte complexes, and a very low-density cell fraction (1.061-density fraction), accounting for approximately 1% to 3% of the starting cell population, was obtained by centrifugation at 1700g for 10 minutes, and washed twice in PBS-EDTA-FCS.

A DC-enriched cell fraction was then obtained after depletion of T cells, B cells, and granulocytes by treating the 1.061-density fraction for 50 minutes at 4°C with a monoclonal antibody (mAb) mixture including anti-CD3 (clone KT3-1.1), anti-B220 (clone RA3-6B2), and anti-granulocyte antigen Gr1 (clone RB6-8C5). The unwanted cells were then removed magnetically after incubation for 30 minutes at 4°C with anti-rat Ig-coated magnetic beads (Dynabeads, Dynal, Oslo, Norway) at a 7:1 bead-cell ratio. Analysis of CD11c expression revealed that DC-enriched cell fractions, used for flow cytometric analysis, were composed of 50% to 80% DCs, as shown in Figure 1A.

For PCR experiments with day 2 PO-LNs or day 6 MS-LNs, DCs were purified by magnetic cell sorting (MACS) with MACS separation columns (Miltenyi Biotec, Bergisch, Germany) after incubation of the DC-enriched cell fraction with biotinylated anti-CD11c mAbs, followed by streptavidin-conjugated MACS microbeads (Miltenyi Biotec). After reanalysis, the DC fraction had a purity of more than 98% (data not shown).

For PCR experiments with day 6 PO-LNs, CD8⁺ DCs were purified with MACS separation columns after incubation of the DC-enriched cell fraction with biotinylated anti-CD8 α mAbs, followed by streptavidin-conjugated MACS microbeads; CD8⁻ DCs were purified with MACS separation columns after incubation of the DC-enriched cell fraction (depleted of CD8⁺ cells with Dynabeads) with biotinylated anti-CD11c mAbs, followed by streptavidin-conjugated MACS microbeads. After reanalysis, these DC fractions had a purity of more than 98% (data not shown).

Blood DC isolation

Heparinized blood was incubated for 30 minutes at 4°C in an ammonium chloride potassium lysis buffer to remove red blood cells (RBCs), washed twice in PBS-EDTA-FCS, and filtered through a stainless-steel sieve. T cells, B cells, and granulocytes were depleted with magnetic beads as described above; FACS analysis revealed that blood DC-enriched cell fractions, used for phenotypic analysis, were composed of more than 50% CD11c⁺ cells, as shown in Figure 5A.

Blockade of cell migration from the blood to the PO-LNs

Blocking of MMTV(SW)-induced blood cell migration via HEVs was achieved by intravenous injection of purified anti-CD62L (L-selectin) antibodies (clone Mel-14), into mice that were injected 36 hours before with MMTV(SW). These mice were analyzed 36 hours after anti-CD62L treatment, that is, at day 3 after MMTV(SW) injection.

LC migration assays

Control or MMTV(SW)-injected BALB/c mice received $10 \mu\text{L}$ 1% fluorescein isothiocyanate (FITC; Sigma, St Louis, MO) dissolved in 1:1

acetone-dibutyl phthalate on the hind footpad, and were analyzed after 3 days for the presence of FITC⁺ DCs in the draining PO-LNs.

Flow cytometry

Analysis of PO-LN DCs was performed after triple staining with FITC-conjugated anti-CD11c (clone N418), phycoerythrin (PE)-conjugated anti-CD8 α (clone CT-CD8 α , Caltag, San Francisco, CA), and biotin-conjugated anti-CD11b (Mac-1; clone M1/70), anti-DEC-205 (clone NLDC-145), anti-CD4 (clone GK1.5) or antileukocyte function-associated antigen (LFA)-1 α (clone FD441.8) followed by streptavidin-tricolor (Caltag). Blood DCs were analyzed after triple staining with FITC-conjugated anti-CD11c, PE-conjugated antimajor histocompatibility complex (MHC) class II (clone M5/114.15.2, Pharmingen, San Diego, CA), and biotin-conjugated anti-CD11b, anti-DEC-205, anti-CD8 α (clone 53-6.72), anti-CD4, anti-CD86 (B7-2; clone GL1, Pharmingen), anti-CD40 (clone FGK45), anti-F4/80 (clone C1.A3.1), or anti-CD62L (L-selectin; clone Mel-14) followed by streptavidin-tricolor. Detection of FITC⁺ cells was achieved after double staining with PE-conjugated anti-CD11c (Pharmingen) and tricolor-conjugated anti-CD8 α (Caltag). Analyses were performed on a FACSsort instrument (Becton Dickinson, Mountain View, CA).

Electron microscopy

The PO-LNs were fixed with 1% glutaraldehyde and 1% paraformaldehyde in 0.1 M pH 7.6 Sørensen phosphate buffer for 2 hours at 4°C, postfixed with 1% OsO₄ in the same buffer for 1 hour at 4°C, dehydrated in graded acetone solutions, and embedded in Embed-812 (Electron Microscopy Sciences, Washington, PA). Semithin sections (1 μm) were stained with toluidine blue and photographed in a Zeiss Axioskop microscope (Zeiss, Oberkochen, Germany), and ultrathin sections (70-80 nm) were counterstained with uranyl acetate and lead citrate and examined with a Jeol 1010 electron microscope (Jeol, Tokyo, Japan).

PCR analysis of DC infection by MMTV(SW)

DNA isolated from highly purified DCs, obtained from PO-LNs or MS-LNs at the indicated times, was amplified using the MMTV(SW) open reading frame (orf)-specific primers 5'-TGG CAA CCA GGG ACT TAT AGG and 3'-GCG ACC CCC ATG AGT ATA TTT, yielding a 316-kb PCR product. PCR was performed on a GeneAmp PCR System 9700, using 2.5 U AmpliTaq Gold polymerase per PCR reaction (Perkin-Elmer, Foster City, CA). PCR conditions were 10 minutes at 95°C, followed by 40 cycles of 30 seconds at 94°C, 30 seconds at 62°C, and 30 seconds at 72°C, and finally 7 minutes at 72°C. PCR products were analyzed on agarose gels stained with ethidium bromide and photographed with a Nikon Coolpix 950 digital camera (Nikon, Tokyo, Japan).

Results

Changes in the PO-LN DC subsets after MMTV(SW) injection

During the first week after injection of MMTV(SW) in the rear footpad of BALB/c mice, important changes occurred in the relative proportions corresponding to the different DC subsets present in the PO-LNs, as illustrated in Figure 1A. As previously described for pooled peripheral LNs,⁴ 3 DC subsets can be defined in the PO-LNs of control mice on the basis of the CD11c versus CD8 α expression, namely CD8⁻, CD8^{int}, and CD8⁺ DCs, which represented around 15%, 75%, and 10% of total PO-LN DCs, respectively. Injection of MMTV(SW) determined a strong increase in the percentage of both CD8⁻ and CD8⁺ subsets, constituting around 70% and 25%, respectively, at day 6. This was paralleled by a dramatic reduction in the percentage of CD8^{int} DCs that constituted around 10% of total DCs at this time. The analysis of the absolute DC number within each PO-LN subset (Figure 2) revealed that the variations in the relative proportion of these DC

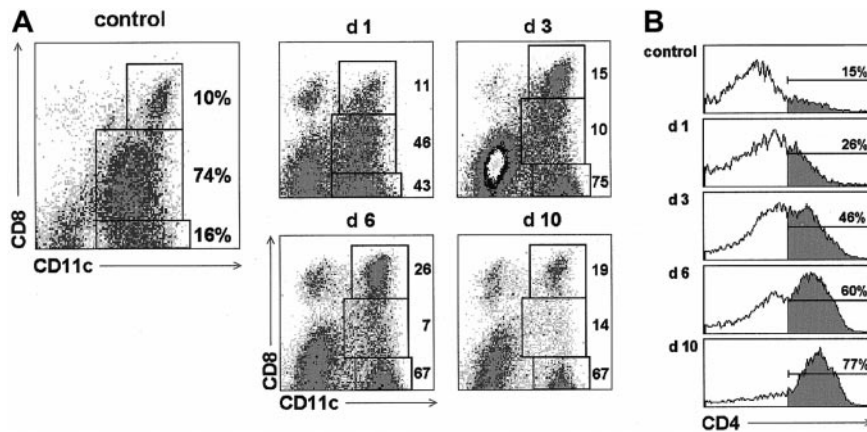


Figure 1. Changes in the PO-LN DC subsets after MMTV(SW) injection. (A) CD11c versus CD8 α profiles of PO-LN DC-enriched cell suspensions at the indicated times after MMTV(SW) injection. The relative percentages represented by CD8 $^{-}$, CD8 int , and CD8 $^{+}$ DC subsets within the total PO-LN DC population are indicated. (B) Variations in the expression of CD4 by PO-LN CD8 $^{-}$ DCs after MMTV(SW) injection. The percentage of CD4 $^{+}$ cells within CD8 $^{-}$ DCs is indicated. Data are representative of 4 experiments with similar results.

subsets induced by MMTV(SW) injection were the result of a considerable augmentation of the CD8 $^{-}$ and CD8 $^{+}$ DC number during the first week after injection, whereas the absolute number of CD8 int DCs did not undergo significant variations. By day 3, approximately a 20- and 7-fold increase in CD8 $^{-}$ and CD8 $^{+}$ DC number was induced by virus injection. By day 6, the cell number increase was 45- and 30-fold for CD8 $^{-}$ and CD8 $^{+}$ DCs, respectively, corresponding to approximately an 18-fold increase in the total DC number at this time. Interestingly, the increase in the absolute number of B cells and T cells was approximately 14- and 4-fold, respectively, at day 3, and 25- and 12-fold at day 6 (data not shown). Therefore, the increase in the number of DCs, specially of the CD8 $^{-}$ subset, induced by MMTV(SW) was significantly higher than the increase of B or T cells, despite the fact that both lymphocyte subsets underwent a strong proliferative response during MMTV(SW) infection.^{7,9} This increase in DC number was concomitant with the presence of high numbers of DCs in the outer cortex of the PO-LNs, in close association with HEVs, as revealed

by light and electron microscopy (Figure 3). DCs were almost undetectable in control PO-LN sections (not shown).

By day 10 an important reduction in all the DC subsets was detected, which corresponded to the extinction of the immune response against MMTV(SW), occurring during the second week after virus injection.⁷ Interestingly, the comparison of the increase in the absolute number of CD8 $^{-}$ versus CD8 $^{+}$ DCs revealed that during the first week the increase was higher for CD8 $^{-}$ than for CD8 $^{+}$ DCs, at all the time points analyzed. These data are in agreement with other results presented later in this report supporting that CD8 $^{+}$ DCs derive from the CD8 $^{-}$ DC subset.

The study of the kinetics of the different PO-LN DC subsets after MMTV(SW) injection described above was performed together with an analysis of the expression of a number of DC markers that have been proven to be decisive in the definition of mouse DC subpopulations, such as CD11b (Mac-1), DEC-205, CD4, and LFA-1.^{4,10,11} No significant phenotypic differences were noticed after virus challenge regarding these markers, except for the expression of CD4 by the CD8 $^{-}$ DC subset. As shown in Figure 1B, only a small proportion of CD8 $^{-}$ DCs were CD4 $^{+}$ in resting PO-LNs, but this marker was strongly up-regulated after MMTV(SW) injection, up to 70% of the cells being positive for this marker by day 6, as described for control CD8 $^{-}$ splenic DCs.²

Blockade of MMTV(SW)-induced increase of PO-LN DC number by anti-CD62L treatment

Because DCs are considered to be nondividing cells once they have reached peripheral lymphoid organs, the increase in DC number after MMTV(SW) injection could reflect a massive entry of DCs to the PO-LNs. The fact that this increase affected CD8 $^{-}$ and CD8 $^{+}$ DCs, but not CD8 int DCs, which in the case of peripheral LN CD8 int DCs have been demonstrated to derive from epidermal LCs,⁴ indicated that MMTV(SW) injection most likely caused the recruitment of DCs from the bloodstream via HEVs. To test this hypothesis, 36 hours after virus challenge, mice were injected with purified anti-CD62L antibodies (clone Mel-14), which block leukocyte migration through HEVs.¹² These mice were analyzed 36 hours later, that is, at day 3 after MMTV(SW) injection. As illustrated in Figure 4, anti-CD62L treatment caused an almost complete inhibition of the increase in CD8 $^{-}$ and CD8 $^{+}$ DC number induced by MMTV(SW), whereas the CD8 int DC subset remained unaffected. This result suggested that a massive entry of blood DCs via HEVs, responsible for the rise in PO-LN DC number, was induced by MMTV(SW), and revealed that this occurred by a CD62L-dependent mechanism.

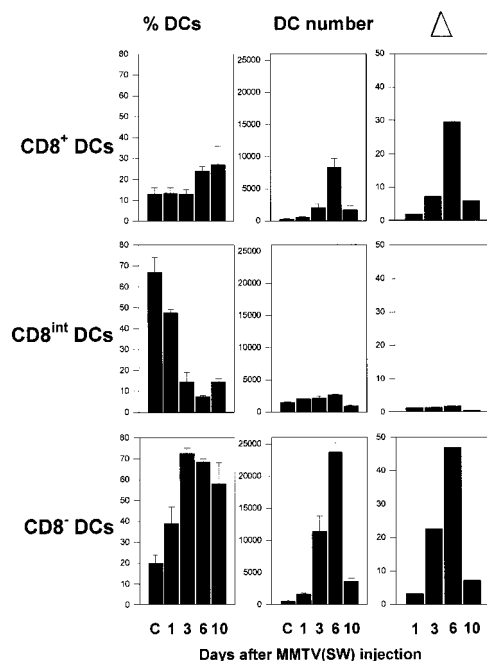
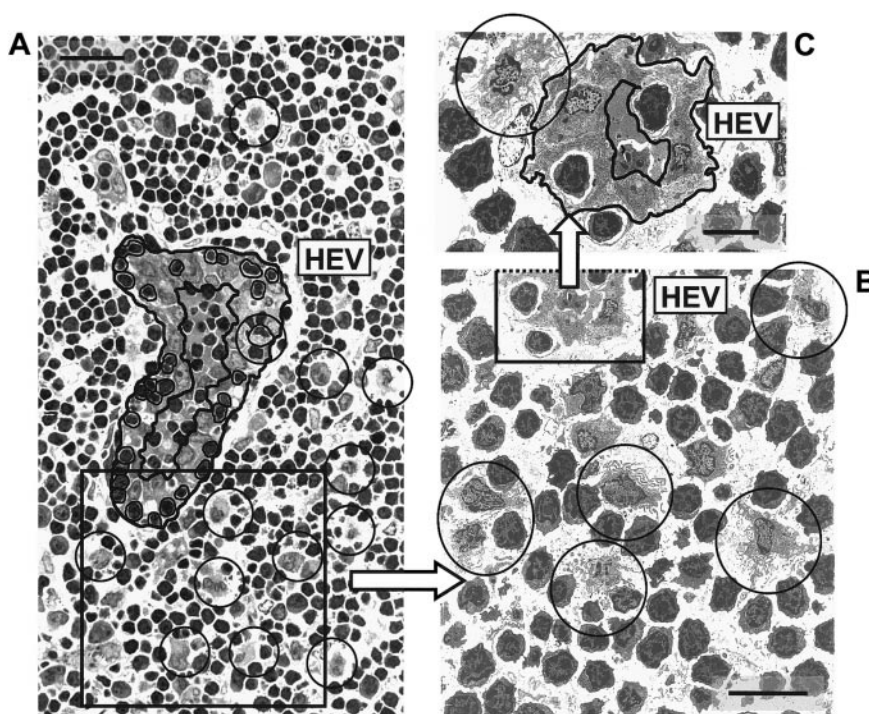


Figure 2. Kinetics of DC subpopulations during infection by MMTV(SW). Histograms illustrate the variations in the relative percentage, absolute DC number, and increase in the absolute cell number (Δ) compared to control PO-LNs, in the CD8 $^{-}$, CD8 int , and CD8 $^{+}$ DC subsets, at the indicated times after MMTV(SW) injection. Data represent the mean \pm SD (n = 4).

Figure 3. Microscopic analysis of PO-LN DCs after MMTV(SW) injection. (A) Semithin section of the outer cortex of the PO-LN at day 6 after MMTV(SW) injection showing a high number of DCs (encircled) around a HEV. The luminal and basal surfaces of the HEV have been marked with a large line. Cells migrating through the HEV have been marked with a fine line. Note the presence of a DC migrating through the HEV. Scale bar = 20 μ m. (B) Electron micrograph of an area similar to the box in panel A, showing numerous DCs in the vicinity of a HEV. Note their complex cell surface processes reflecting a highly migratory state. Scale bar = 10 μ m. (C) DC in contact with the basal surface of a HEV. Enlargement of an area similar to the box shown in panel B. Scale bar = 5 μ m.



To further define MMTV(SW)-induced DC recruitment to the LNs, an analysis of blood DC phenotype was performed, because to our knowledge mouse blood DCs had not been previously characterized. For this purpose, a DC-enriched cell suspension was obtained from BALB/c mice, after treatment of heparinized blood with lysis buffer, followed by magnetic bead depletion, as described in "Materials and methods." Blood DCs, defined as CD11c⁺ cells, displayed a pattern of cell surface marker expression resembling that previously reported for spleen and LN CD8⁻ DCs,^{2,4} that is, CD11b (Mac-1)⁺, DEC-205^{low}, CD8 α ⁻, CD86 (B7.2)⁺, CD40⁺, F4/80⁺ (Figure 5). Interestingly, in contrast to splenic CD8⁻ DCs, blood DCs did not express CD4, and about 50% of them expressed CD62L.

In conclusion, because MMTV(SW) induced the entry to the LN of blood DCs, negative for CD8, leading to an increase not

only of CD8⁻ DCs but also of the CD8⁺ DC subset, our data support the view that CD8⁺ DCs originate from CD8⁻ DCs by a differentiation or maturation process involving the up-regulation of the CD8 molecule.

Inhibition of LC migration to the draining LNs during MMTV(SW) infection

With regard to CD8^{int} DCs, as mentioned above, this DC subset did not undergo significant variations after MMTV(SW) injection and, on the other hand, anti-CD62L treatment did not determine significant variations in the absolute cell number within this population. These data suggest that PO-LN CD8^{int} DCs do not derive from blood-borne DCs, but rather that they gain access to the PO-LNs via afferent lymphatics, in agreement with previous data from our group⁴ demonstrating that CD8^{int} DCs located in auricular LNs derive from ear epidermal LCs.

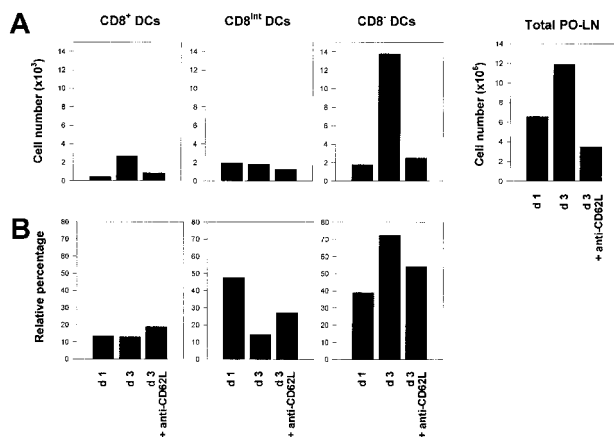


Figure 4. Blocking of DC migration via HEVs. (A) Histograms represent the absolute cell number of PO-LN CD8⁺, CD8^{int}, and CD8⁻ DCs, as well as the total number of PO-LN cell number, at day 1 or 3 after MMTV(SW) injection, and of mice injected intravenously with anti-CD62L mAb at day 1 after MMTV(SW) injection and analyzed at day 3. (B) Relative percentage of PO-LN CD8⁺, CD8^{int}, and CD8⁻ DCs for the same experimental condition described for panel A. Data are representative of 2 experiments with similar results.

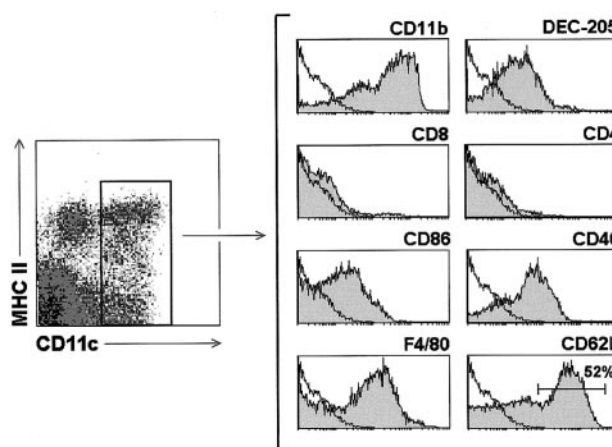


Figure 5. Phenotypic analysis of blood DCs. Gray profiles correspond to the expression of the indicated markers by blood DCs after gating for CD11c⁺ cells. White profiles represent control stainings. Data are representative of 5 experiments with similar results.

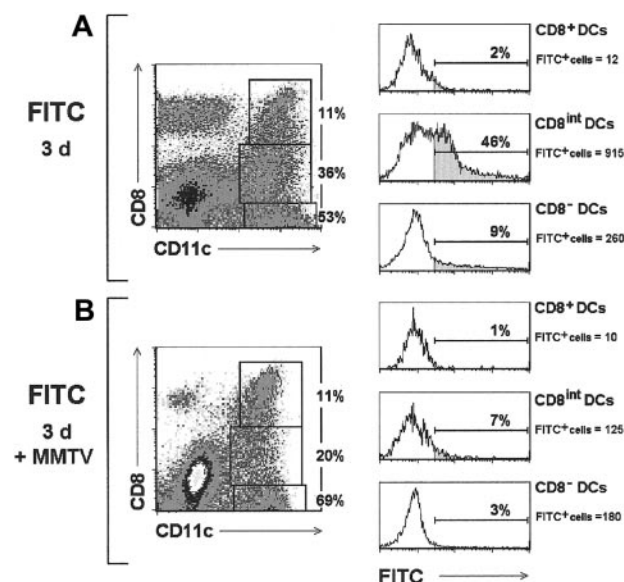


Figure 6. Inhibition of LC migration by MMTV(SW). Contour plots correspond to the PO-LN CD11c versus CD8 profiles of control mice or MMTV(SW)-injected mice, analyzed 3 days after FITC-labeling of the hind footpad epidermis. The relative proportion of CD8⁻, CD8^{int}, and CD8⁺ DC subsets is indicated. Histograms show FITC labeling of the indicated DC subsets after defining the corresponding gates in the contour plots. The percentage and absolute cell number per PO-LN of FITC⁺ cells is indicated for each DC population. Data are representative of 3 experiments with similar results.

To test whether this was the case, the rear footpad of BALB/c mice was labeled with a FITC solution, and the PO-LNs analyzed after 3 days. As expected, FITC⁺ DCs were found mainly within the CD8^{int} DC subset (Figure 6A), where they represented up to 45% of the cells (approximately 900 CD8^{int} FITC⁺ DCs per PO-LN in the experiment illustrated in Figure 6), confirming that these cells derived from LCs that had migrated to the PO-LN. The CD8⁻ DC population contained around 10% FITC⁺ cells (approximately 250 CD8⁻ FITC⁺ DCs per PO-LN in the experiment illustrated in Figure 6), most likely corresponding to LCs that had reached the LNs but had not up-regulated the CD8 molecule yet. Only 2% FITC⁺ cells were found within CD8⁺ DCs, which probably corresponded to FITC⁺ CD8^{int} DCs included in the CD8⁺ DC analysis gate. Interestingly, when this migration assay was performed in mice that had been injected with MMTV(SW) prior to FITC labeling of the epidermis, the proportion of FITC⁺ DCs was strongly reduced (Figure 6B), because only 7% and 3% FITC⁺ cells were found within the CD8^{int} and CD8⁻ DC subsets, respectively (approximately 120 and 180 FITC⁺ DCs per PO-LN within the CD8^{int} and CD8⁻ DC subsets, respectively, in the experiment illustrated in Figure 6). No significant numbers of FITC⁺ cells were detected in these mice within the CD8⁺ DC subpopulation. These results suggest that MMTV(SW) injection created a blockade in LC migration to the draining LNs.

PCR analysis of DC infection by MMTV(SW)

The data presented in this report revealed that during the infection by MMTV(SW), the PO-LN DCs underwent profound variations involving a massive recruitment of DCs via HEVs. On the other hand, in a recent report, the involvement of DCs in early phases of MMTV(SW) infection has been suggested,¹³ although no direct evidence of DC infection by MMTV has been reported yet. On the basis of these results we have investigated whether PO-LN DCs become infected after MMTV(SW) injection. For this purpose, highly purified DCs were analyzed for the presence of MMTV(SW)

DNA after integration in the target cell genome by PCR, using primers specific for MMTV(SW). To address whether DCs were infected during the early phases of the process of MMTV(SW) infection, when the first infected B cells can be detected,¹⁴ PO-LN DCs were purified from mice injected 48 hours before with the virus. To test whether CD8⁻ or CD8⁺ DCs (or both) were infected, these DC subsets were purified from PO-LNs, 6 days after virus injection. Our results, shown in Figure 7, demonstrate that MMTV(SW) DNA can be detected in DCs from day 2 PO-LNs, and in both CD8⁻ and CD8⁺ DCs isolated from day 6 PO-LNs, but not in DCs isolated from day 6 MS-LNs, used as control DCs. These data support that DCs could participate in the first phases of MMTV(SW) infection, as previously proposed.¹³ Finally, the fact that both CD8⁻ and CD8⁺ DCs were infected at later phases of the infection process, suggest that DCs could be involved in viral transmission to the mammary gland, as described for extrafollicular plasmablasts.⁷

Discussion

The immune response against MMTV involves a strong B-cell proliferative response that determines the amplification of the few initially infected B cells, required for an efficient infection process leading ultimately to the transmission of MMTV to the mammary gland and to the progeny.¹⁵ Previous studies using an experimental MMTV infection model, in which the immune response against MMTV can be analyzed in the PO-LNs after virus injection into the hind footpad of BALB/c mice, revealed that MMTV determined an inflammatory response in the PO-LN causing the influx of B and T cells from the bloodstream via HEVs.^{7,9}

In the present study, we have analyzed the behavior of the PO-LN DC subsets during the infection by MMTV(SW). Injection of MMTV(SW) induced a massive increase in the number of DCs in the PO-LN caused by the entry of blood-borne DCs. Although it has been previously reported that Rauscher leukemia virus infection was accompanied by an increase in peripheral LN DCs,¹⁶ our

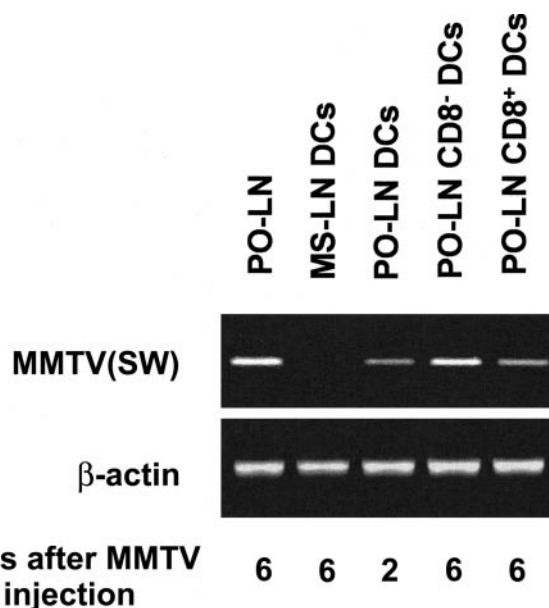


Figure 7. PCR analysis of DC infection by MMTV(SW). The indicated DCs subsets purified from day 2 or day 6 PO-LNs were analyzed by PCR for the presence of MMTV(SW) DNA using specific primers. Day 6 total PO-LN cells and purified MS-LN DCs were used as positive and negative controls, respectively.

data provide the first evidence of a massive DC recruitment from the blood to the LNs via HEVs driven by an inflammation/viral infection process. In addition, our blocking experiments using anti-CD62L mAbs demonstrated that DC recruitment to the LNs occurred by a CD62L-dependent mechanism, as previously shown for lymphocytes and granulocytes,¹² but not for DCs. Interestingly, whereas DCs located extravascularly in lymphoid organs such as the spleen, Peyer patches, and thymus do not express the homing receptor CD62L,⁴ which has been demonstrated to be involved in leukocyte migration to peripheral LNs via HEVs,¹² around 50% of blood CD11c⁺ DCs expressed this molecule, which, as shown here, participates in DC recruitment to the LNs. Concerning CD4 expression, blood DCs are negative for this marker, whereas about 70% of splenic DCs are CD4⁺.² However, although control PO-LN CD8⁻ DCs did not express CD4, this molecule was up-regulated by these cells after MMTV(SW) injection, concomitantly with their increase in cell number. These data may reflect a CD8⁻ DC differentiation or activation process that would involve CD4 up-regulation. In this sense we have previously reported CD4 up-regulation by splenic CD8⁻ DCs during DC reconstitution after irradiation and the down-regulation of CD4 by splenic CD8⁻ after culture in the presence or absence of mAbs against CD40 or CD43, known to induce DC activation.²

With regard to the different PO-LN DC subsets, in control mice the majority of DCs correspond to the LN-related subset of CD8^{int} DCs,^{4,17} which has been claimed to derive from epidermal LCs in the case of peripheral LNs CD8^{int} DCs, and from intestinal lamina propria DCs for MS-LN CD8^{int} DCs (F.A., manuscript in preparation). During the infection process by MMTV(SW) a strong increase in the absolute number of CD8⁻ and CD8⁺ PO-LN DCs occurred, whereas the CD8^{int} DC subpopulation did not undergo significant variations. This resulted in a progressive reduction in the percentage represented by this subset, and consequently at the peak of the immune response against MMTV(SW), that is, by day 6 after virus injection, CD8^{int} DCs represented less than 10% of total PO-LN DCs, whereas CD8⁻ and CD8⁺ DCs constituted around 70% and 15%, respectively. In addition, experiments of CD62L blocking did not affect the CD8^{int} DC population, supporting that these cells do not get access to the PO-LNs via HEVs, but rather from the skin via afferent lymphatics, as proposed above. Our LC migration studies confirmed this hypothesis and in addition suggested that MMTV(SW) infection caused the inhibition of epidermal LC migration. In this regard, blockade of LC migration by viral infection has been previously reported for Rauscher leukemia virus infection.¹⁶ In conclusion, the increase in PO-LN occurring during MMTV(SW) infection affected the CD8⁻ and CD8⁺ DC subsets, but not CD8^{int} DCs. In addition, for all the time points analyzed the number of CD8⁻ DCs was significantly higher than that of CD8⁺ DCs. On the other hand, our data support that this increase is the result of the recruitment of blood-borne DCs, not expressing CD8, via HEVs. In this sense, MMTV(SW)-induced DC recruitment to the PO-LNs is probably under the control of chemokines involved in inflammatory responses during viral infections, such as macrophage inflammatory protein 1 α (MIP-1 α), which has been demonstrated to mediate inflammatory chemotactic processes during viral infections.¹⁸ Interestingly, immature DCs express the chemokine receptor for MIP-1 α , CCR5,¹ and it has been reported recently that CCR5 can trigger interleukin 12 production by mouse splenic DCs.¹⁹

Taken together these data support the hypothesis that DC recruitment from the blood determined an augmentation of the CD8⁻ DC subset, and subsequently that CD8⁻ DCs would generate

CD8⁺ DCs by a differentiation/maturation process, resulting in an increase of the CD8⁺ DC subset.

The concept that the generation of CD8⁺ DCs is the result of a CD8⁻ DC maturation process, contrasts with the widely accepted hypothesis that CD8⁻ and CD8⁺ DCs might represent different DC lineages, specifically myeloid- and lymphoid-derived DCs, respectively. However, this concept has been recently challenged by our data,² demonstrating that both DC subsets can be generated from the CD4^{low} lymphoid-committed precursor population. These data were subsequently extended in 2 recent reports showing that CD8⁻ and CD8⁺ DCs could be derived from either lymphoid- or myeloid-committed precursors.^{3,20} Consequently, these new data reopen the problem of the correlation between mouse CD8⁻ and CD8⁺ DCs and their origin. In this sense, the possibility that CD8⁺ DCs could derive from CD8⁻ DCs on maturation was proposed previously by Shortman and colleagues, but rapidly rejected due in part to the negative results obtained in experiments conducted to test whether CD8 expression could be induced in CD8⁻ DCs in vitro.^{11,17,21} In addition, the fact that in preliminary experiments CD8⁺ DCs but not CD8⁻ DCs were found within the progeny of lymphoid precursors on transfer into irradiated recipients, led to the concept that they represented unrelated DC subpopulations.²² Moreover, no experimental evidence refutes the hypothesis that CD8⁺ DCs are a mature form of the CD8⁻ DCs, but rather a number of experimental data support it. In this regard, it has been shown that splenic CD8⁻ DCs are located around the white pulp in relation with the marginal zone, whereas CD8⁺ DCs are found in the inner white pulp.²³ Interestingly, bacterial lipopolysaccharide or soluble *Toxoplasma gondii* tachyzoite antigen (STAg), known to promote DC maturation, causes splenic CD8⁻ DC migration toward the inner white pulp, where CD8⁺ DCs are located,²³ and this is paralleled by the up-regulation of DEC-205,^{24,25} described as an endocytic receptor expressed in vivo or ex vivo by CD8⁺ but not by CD8⁻ DCs.¹⁷ Similar observations, supporting the CD8 up-regulation on CD8⁻ DC maturation, were reported by analyzing Peyer patch CD8⁻ DC migration from the subepithelial dome to the interfollicular T-cell areas, induced by intravenous administration of STAg.²⁶ Therefore, the hypothesis of CD8⁺ DC generation by a CD8⁻ DC maturation process involving the up-regulation of CD8 is strongly supported by the data presented here, and is further strengthened by the data reported above.

Finally, on the basis of a previous report¹³ claiming for an essential role of DCs in the early phases of infection by MMTV(SW), we investigated whether DCs were infected by MMTV. Our results revealed that DCs were infected by MMTV(SW) in the 48 hours after virus injection, providing the first evidence of DC infection by MMTV. With regard to the participation of DCs in viral infections, it has been demonstrated that DCs play an essential role in the induction of the antiviral immune response against HIV, by acting as initiators of the activation of virus-specific T cells and more importantly, in HIV transport and dissemination.²⁷ In addition, DCs have been claimed to be involved in the pathogenesis/response to a variety of viruses, such as cytomegalovirus, measles virus, herpes virus, influenza virus, and respiratory syncytial virus.¹ In this sense, the demonstration that PO-LN DCs are infected in the early phases of the infection by MMTV(SW) could be related with their presumed role of induction of the immune response against this virus, because DCs have been demonstrated to be capable of presenting efficiently MMTV(SW) superantigens to specific T cells.^{28,29} Moreover, the fact that both CD8⁻ and CD8⁺ DCs become infected by MMTV(SW) at later phases of infection, suggests that DCs could

participate in the spreading of MMTV infection and subsequent transmission to the mammary gland, which still remain specially controversial issues in MMTV infection.

In conclusion, our data derived from the study of DCs during the infection by MMTV(SW) provide the first evidence of DC recruitment from the blood via HEVs by a CD62L-dependent mechanism, as the result of a viral infection-induced inflammatory response. In addition they strongly support a functional correlation between CD8⁻ and CD8⁺ DCs and demonstrate that DCs are infected by MMTV(SW). Additional experiments are being conducted in our laboratory to determine the chemokine-driven

mechanisms involved in DC recruitment induced by MMTV and the role of DCs in the infection by this retrovirus.

Acknowledgments

The authors would like to thank Dr H. Acha-Orbea (Ludwig Institute for Cancer Research, Lausanne, Switzerland) for the MMTV-specific primers and Dr A. Rolink (Basel Institute for Immunology, Basel, Switzerland) for the anti-CD40 hybridoma FGK45.

References

- Banchereau B, Briere F, Caux C, et al. Immunobiology of dendritic cells. *Annu Rev Immunol*. 2000; 18:767-811.
- Martín P, Martínez del Hoyo G, Anjuère F, et al. Concept of lymphoid versus myeloid dendritic cell lineages revisited: both CD8 α ⁻ and CD8 α ⁺ dendritic cells are generated from CD4^{low} lymphoid-committed precursors. *Blood*. 2000;96:2511-2519.
- Traver D, Akashi K, Manz M, et al. Development of CD8 α -positive dendritic cells from a common myeloid progenitor. *Science*. 2000;290:2152-2154.
- Anjuère F, Martín P, Ferrero I, et al. Definition of dendritic cell subpopulations present in the spleen, Peyer's patches, lymph nodes and skin of the mouse. *Blood*. 1999;93:590-598.
- Anjuère F, Martínez del Hoyo G, Martín P, Ardavin C. Langerhans cells acquire a CD8⁺ dendritic cell phenotype on maturation by CD40 ligation. *J Leukoc Biol*. 2000;67:206-209.
- Merad M, Fong L, Bogenberger J, Engleman EG. Differentiation of myeloid dendritic cells into CD8 α -positive dendritic cells in vivo. *Blood*. 2000; 96:1865-1872.
- Ardavin C, Martín P, Ferrero I, et al. B cell response after MMTV infection: extrafollicular plasmablasts represent the main infected population and can transmit viral infection. *J Immunol*. 1999; 162:2538-2545.
- Held W, Shakhov AN, Waanders GA, et al. An exogenous mouse mammary tumor virus with properties of Mls-1a (Mtv-7). *J Exp Med*. 1992; 175:1623-1633.
- Ardavin C, Luthi F, Andersson M, et al. Retrovirus-induced target cell activation in the early phases of infection: the mouse mammary tumor virus model. *J Virol*. 1997;71:7295-7299.
- Vremec D, Zorbas M, Scollay R, et al. The surface phenotype of dendritic cells purified from mouse thymus and spleen: investigation of the CD8 expression by a subpopulation of dendritic cells. *J Exp Med*. 1992;176:47-58.
- Vremec D, Pooley J, Hochrein H, Wu L, Shortman K. CD4 and CD8 expression by dendritic cell subtypes in mouse thymus and spleen. *J Immunol*. 2000;164: 2978-2986.
- Girard J-P, Springer TA. High endothelial venules (HEVs): specialized endothelium for lymphocyte migration. *Immunol Today* 1995;16:449-457.
- Baribaud F, Maillard I, Vacheron S, Brocker T, Diggelmann H, Acha-Orbea H. Role of dendritic cells in the immune response induced by mouse mammary tumor virus superantigen. *J Virol*. 1999;73:8403-8410.
- Held W, Shakhov AN, Izui S, et al. Superantigen-reactive CD4⁺ T cells are required to stimulate B cells after infection with mouse mammary tumor virus. *J Exp Med*. 1993;177:359-366.
- Held W, Waanders GA, Shakhov AN, Scarpellino L, Acha-Orbea H, MacDonald HR. Superantigen-induced immune stimulation amplifies mouse mammary tumor virus infection and allows virus transmission. *Cell*. 1993;74:529-540.
- Gabrilovich DI, Woods GM, Patterson S, Harvey JJ, Knight SC. Retrovirus-induced immunosuppression via blocking of dendritic cell migration and down-regulation of adhesion molecules. *Immunology*. 1994;82:82-87.
- Vremec D, Shortman K. Dendritic cell subtypes in mouse lymphoid organs: cross-correlation of surface markers, changes with incubation, and differences among thymus, spleen, and lymph nodes. *J Immunol*. 1997;159:565-573.
- Cook DN, Beck MA, Coffman TM, et al. Requirement of MIP-1 α for an inflammatory response to viral infection. *Science*. 1995;269:1583-1585.
- Aliberti J, Reis e Sousa C, Schito M, Hieny S, Wells T, Huffnagle GB. CCR5 provides a signal for microbial induced production of IL-12 by CD8 α dendritic cells. *Nat Immunol*. 2000;1:83-87.
- Manz MG, Traver D, Miyamoto T, Weissman IL, Akashi K. Dendritic cell potentials of early lymphoid and myeloid progenitors. *Blood*. 2001;97: 3333-3341.
- Kamath AT, Pooley J, O'Keeffe M, et al. The development, maturation, and turnover rate of mouse spleen dendritic cell populations. *J Immunol*. 2000;165:6762-6770.
- Wu L, Li CL, Shortman K. Thymic dendritic cell precursors: relationship to the T lymphocyte lineage and phenotype of the dendritic cell progeny. *J Exp Med*. 1996;184:903-911.
- Leenen PJM, Radosevic K, Voerman JSA, et al. Heterogeneity of mouse spleen dendritic cells: in vivo phagocytic activity, expression of macrophage markers, and subpopulation turnover. *J Immunol*. 1998;160:2166-2173.
- De Smedt T, Pajak B, Muraille E, et al. Regulation of dendritic cell numbers and maturation by lipopolysaccharide in vivo. *J Exp Med*. 1996;184: 1413-1424.
- Reis e Sousa C, Hieny S, Schariton-Kersten T, et al. In vivo microbial stimulation induces rapid CD40 ligand-independent production of interleukin 12 by dendritic cells and their redistribution to T cell areas. *J Exp Med*. 1997;186:1819-1829.
- Iwasaki A, Kelsall BL. Localization of distinct Peyer's patch dendritic cell subsets and their recruitment by chemokines macrophage inflammatory protein (MIP)-3 α , MIP-3 β , and secondary lymphoid organ chemokine. *J Exp Med*. 2000;191: 1381-1393.
- Sewell AK, Price DA. Dendritic cells and transmission of HIV-1. *Trends Immunol*. 2001;22:173-175.
- Ardavin C, Waanders GA, Ferrero I, Anjuère F, Acha-Orbea H, MacDonald HR. Expression and presentation of viral superantigens by thymic and splenic dendritic cells and B cells. *J Immunol*. 1996;157:2789-2794.
- Ferrero I, Anjuère F, MacDonald HR, Ardavin C. In vitro negative selection of viral superantigen-reactive thymocytes by thymic dendritic cells. *Blood*. 1997;90:1943-1951.